New complex permeability measurement device for thin magnetic films

S. Hayano, I. Marinova, and Y. Saito
College of Engineering, Hosei University, Kajino, Koganei, Tokyo 184, Japan

Previously, we have proposed a strategic dual image (SDI) method to obtain the finite element solution of open boundary magnetic field problems. Also, we have derived a complex permeability from a Chua-type magnetization model. Combination of this complex permeability with the SDI method is now applied to exploit a new high frequency characteristic measurement device for thin magnetic films. Numerical simulation suggests that our new measurement method yields far superior results compared with those of the conventional one.

I. INTRODUCTION

At high frequency, the peak flux density in the magnetic materials is sufficiently small that both the flux density and field intensity are sinusoidally time varying. This makes it possible to employ a complex permeability representing the magnetization characteristics. Previously, we proposed a Chua-type magnetization model based on the magnetic domain theory.[1–5] Also, this Chua-type model was successfully applied to derive a complex permeability.[6]

In the present paper, we propose one of the novel methods for measuring the complex permeability of thin magnetic films. The measurement principle of the conventional method is that the mean flux density B in a specimen is obtained from a difference linkage flux between the detection and correction coils; and the field H is obtained from linkage flux of the detection coil. Each of the coils of the conventional measurement method is that the detection and correction coils are arranged in parallel in the exciting coil. In the new method, the detection, correction, and exciting coils are coaxially arranged in each other, and the flux density B is similarly obtained as those of the conventional one, but field intensity H in a specimen can be obtained by extrapolating the field intensities in the outer and inner detection coils. According to the simulation in the two-dimensional (2D) as well as axisymmetric coordinate systems, it is suggested that the new method yields the extremely higher accurate results compared with those of the conventional one.

II. FINITE ELEMENT SOLUTION OF OPEN BOUNDARY HYSTERETIC FIELDS

A. Complex permeability

At high frequency, it is possible to assume that both the flux density and field intensity are sinusoidally time varying. This is because the peak flux density in the magnetic materials is sufficiently small. Thus, it is possible to employ a complex permeability representing the magnetization characteristics. Previously, we proposed a Chua-type magnetization model based on the magnetic domain theory.[1–5] Also, this Chua-type model was successfully applied to derive a complex permeability.[6] A Chua-type magnetization model is given by

$$H+(\mu_r/s)dH/dt=(1/\mu)B+(1/s)dB/dt, \tag{1}$$

where H, B, μ, μ_r, and s are the field intensity, flux density, permeability, reversible permeability, and hysteresis coefficient, respectively.[1–5] These parameters can be assumed to take the constant values when the flux density B as well as the field intensity H are sinusoidally time varying. When we employ a complex notation $d/dt=j\omega$, the complex permeability $\mu(\omega)$ is derived from Eq. (1) as

$$\mu(\omega)=B/H=\mu_R(\omega)-j\mu_I(\omega)=\mu[(s^2+\omega^2\mu\mu_r)/(s^2+\omega^2\mu^2)]-j\mu\omega s[(\mu-\mu_r)/(s^2+\omega^2\mu^2)], \tag{2}$$

where $j=\sqrt{-1}$; $\omega=2\pi f$ (f:frequency). Figure 1 shows an example of the frequency characteristics of the complex permeability.

B. Strategic dual image method

For simplicity, let us consider a 2D magnetic field problem having an open boundary. The key idea of the strategic dual image (SDI) method is that any vector fields and their field sources, respectively, can be divided into two components: rotational and divergent.[7–10] Thereby, it is possible to exploit a method by which the rotational and divergent components can be obtained by imposing the rotational and divergent field source images, respectively. In magnetic field problems, the rotational and divergent field sources correspond to the current i and magnetic charge m so that the rotational field component can be obtained by imposing the corresponding image current as shown in Fig. 2(a). In this case, the condition

$$\sum_{p=1}^{q}(i_p/r_p)=0 \tag{3}$$

must be satisfied at the center of a circular hypothetic boundary to reduce the net image to zero. In Eq. (3), q and r_p denote the number of source currents and the distance from a center of the hypothetic boundary to the current i_p, respectively. Equation (3) and the image in Fig. 2(a) mean that the total currents in the problem region must be zero, and the vector potentials at the center as well as on the circular hypothetic boundary must be zero. Therefore, the calculation of the rotational field component can be reduced to the solution of a vector potential problem having zero boundary conditions at the circular hypothetic boundary and the center of its

 0021-8979/94/75(10)/6887/3/$6.00

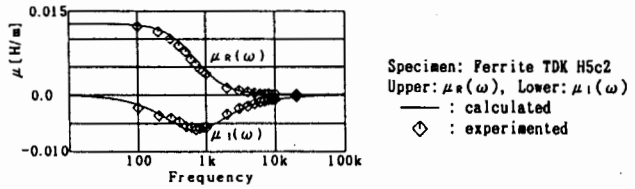

FIG. 1. Frequency characteristics of $\mu_R(\omega)$ and $\mu_I(\omega)$.

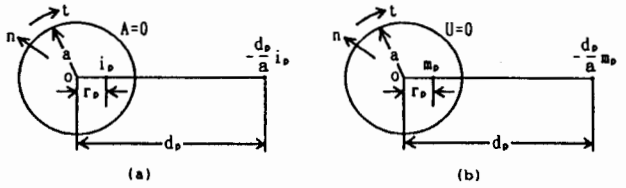

FIG. 2. (a) The rotational field source image $-(d_p/a)i_p$. (b) The divergent field source image $-(d_p/a)m_p$.

hypothetic boundary. Similarly, it is possible to show that the calculation of the divergent field component can be reduced to the solution of a scalar potential problem having zero boundary conditions at the circular hypothetic boundary and the center of the hypothetic boundary, as shown in Fig. 2(b). Obviously, the zero boundary condition of scalar potential U at the hypothetic boundary corresponds to the symmetrical boundary condition of vector potential A. This means, if we employ the vector potential A to represent the open field, then the calculation of the divergent field component may be reduced to the solution of a vector potential problem having the symmetrical boundary condition at the circular hypothetic boundary and the zero boundary condition at the center of the hypothetical boundary. Thus, the open boundary field calculation can be reduced to the solution of zero and the symmetrical boundary problems having the circular hypothetic boundary for two dimensions and the elliptic hypothetic boundary having an axial ratio of 1.8 for axisymmetrical dimensions.[7–11] According to Ref. 11, the axial ratio 1.8 in axisymmetrical dimensions could be determined by considering the demagnetization factor of the elliptic solid. Further, the zero condition must be set at the center of the hypothetic boundary by Eq. (3) for both zero and symmetrical boundary problems.

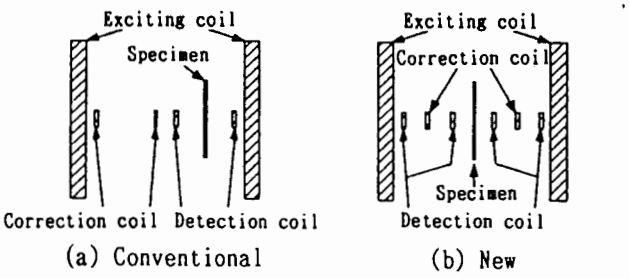

FIG. 3. The 2D models of the measurement devices.

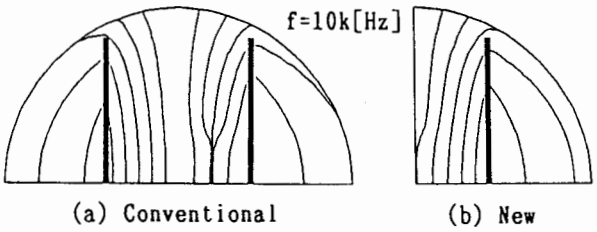

FIG. 4. Field distributions in 2D models. Specimen: TDK H5c2, thickness: 10 (μm), length: 10 (mm), frequency $f=10k$ (Hz).

C. The high frequency measurements for the thin magnetic films

Figure 3 shows the 2D models of a high frequency characteristic measurement device for the thin magnetic films. The measurement principle of the conventional method is that the mean flux density B in a specimen is obtained from a linkage flux difference between the detection and correction coils; and the field H is obtained from the linkage flux of the detection coil. The principle may be correct if the fields in the correction and detection coils distribute in parallel to each of the correction and detection coil axes. However, this condition is not always held but the reasonable field distribution is distorted by the specimen in the detection coil. In order to overcome this difficulty, we propose here a new method. In this new method, the flux density B is similarly obtained as in the conventional one, but the field intensity H in a specimen can be obtained by extrapolating the field intensities in outer and inner detection coils.

Figure 4 shows the examples of the field distribution in 2D models. Obviously, a field of the conventional measurement method becomes asymmetrically distributed, caused by

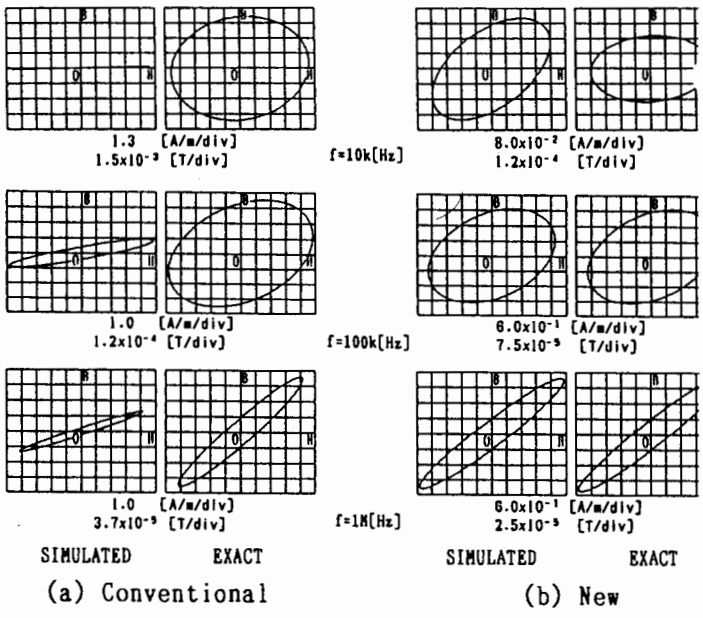

FIG. 5. Hysteresis loops of a thin magnetic film in two dimensions. Specimen: TDK H5c2, thickness: 10 (μm), length: 12 (mm).

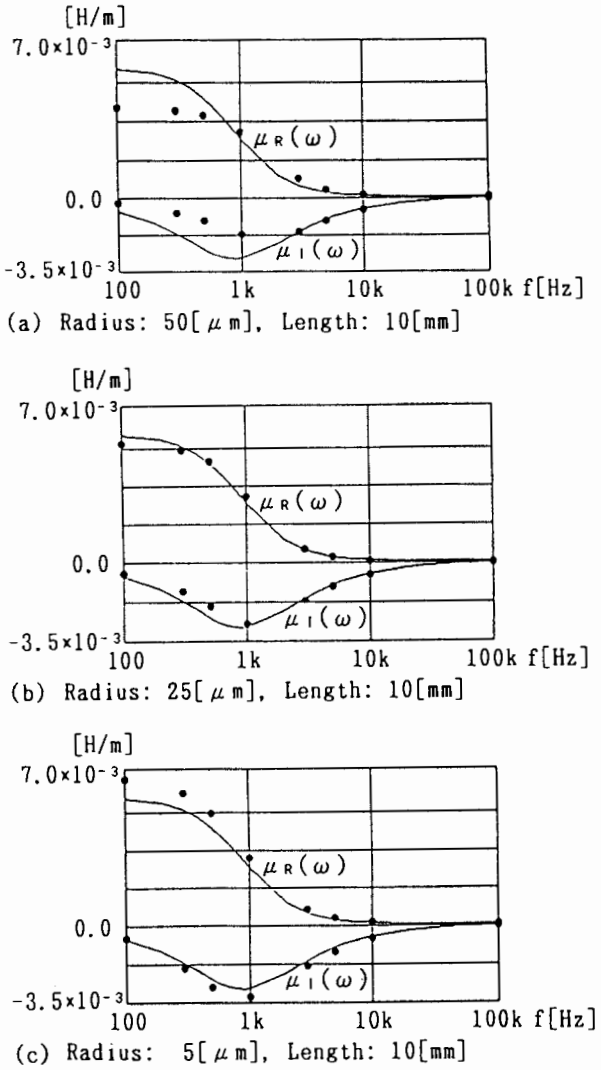

FIG. 6. Frequency characteristics of the complex permeability. Solid lines: exact, solid dots: simulated in the axisymmetrical dimensions assuming the slender magnetic bars instead of thin magnetic films. Specimen: TDK H5c2.

the specimen in the detection coil. On the contrary, a field of the new method becomes symmetrically distributed. This means that it is possible to extrapolate the field intensity H in the material with fairly good accuracy.

Figure 5 shows the comparison between the simulated and exact hysteresis loops in two dimension. The results in Fig. 5 suggest that the new method makes it possible to measure the high and low frequency characteristics of the thin films with higher accuracy.

As shown in Fig. 6, even if the axisymmetrical coordinate system assumes the slender magnetic bars instead of thin magnetic films, it is obvious that the new method provides fairly good results. Also, it is revealed that the measured accuracy becomes higher for slender magnetic bars. This is because the magnetic field distribution in the specimen becomes not uniform for thicker magnetic bars due to the skin effect.

III. CONCLUSION

As shown above, we have shown that the finite element solutions of open boundary hysteretic field problems could be evaluated by combining the SDI method with complex permeability. As an application of our method, the new high frequency characteristic measurement device for the thin magnetic films has been developed to get more accurate results compared with those of the conventional one.

ACKNOWLEDGMENT

The authors gratefully acknowledge A. Miyazaki of the IWATSU Co. LTD. for his practical coding works.

[1] Y. Saito, S. Hayano, Y. Kishino, K. Fukushima, H. Nakamura, and N. Tsuya, IEEE Trans. Magn. **MAG-22**, 647 (1986).
[2] Y. Saito, K. Fukushima, S. Hayano, and N. Tsuya, IEEE Trans. Magn. **MAG-23**, 2227 (1987).
[3] Y. Saito, S. Hayano, and Y. Sakaki, J. Appl. Phys. **64**, 5684 (1988).
[4] Y. Saito, M. Namiki, S. Hayano, and N. Tsuya, IEEE Trans. Magn. **MAG-25**, 2986 (1989).
[5] Y. Saito, M. Namiki, and S. Hayano, J. Appl. Phys. **67**, 4738 (1990).
[6] S. Hayano, A. Miyazaki, and Y. Saito, J. Appl. Phys. **69**, 4838 (1991).
[7] Y. Saito, K. Takahashi, and S. Hayano, IEEE Trans. Magn. **MAG-23**, 3569 (1987).
[8] Y. Saito, K. Takahashi, and S. Hayano, J. Appl. Phys. **63**, 3366 (1988).
[9] Y. Saito, K. Takahashi, and S. Hayano, IEEE Trans. Magn. **MAG-24**, 2946 (1988).
[10] Y. Saito, K. Takahashi, and S. Hayano, *Proceedings of First International Symposium on Applied Electromagnetics in Materials* (Pergamon, New York, 1989), p. 237.
[11] K. Takahashi, Y. Saito, and S. Hayano, *International Journal of Applied Electromagnetics in Materials* (Elsevier, Amsterdam, 1993), p. 179.